

## The Application of RADARSAT-2 Quad-Polarized Data for Oil Slick Characterization

Gordon Staples<sup>1</sup> and Ridha Touzi<sup>2</sup>

1. MDA Geospatial Services Inc.  
13800 Commerce Parkway, Richmond, BC, V6V 2J3  
[gstaples@mdacorporation.com](mailto:gstaples@mdacorporation.com)

2. CCRS  
588 Booth St., Ottawa, ON, K1A 0Y7  
[rtouzi@NRCan-RNCan.gc.ca](mailto:rtouzi@NRCan-RNCan.gc.ca)

**ABSTRACT 300300:**

Spaceborne radar data has been extensively used to monitor numerous oil spills worldwide. The radar imagery provides information on the spatial extent of the oil, but in general, there is limited information on the characteristics of the oil such as the discrimination of sheen from emulsion. The full polarimetry capabilities of RADARSAT-2 were investigated in this study using acquisitions collected over the Gulf of Mexico. In this study, the Cloude-Pottier target decomposition algorithm was used to extract polarimetric information from RADARSAT-2 quad-polarized images acquired over the Macondo oil spill in the Gulf of Mexico. The Cloude-Pottier entropy ( $H$ ) provides a measure of the amount of mixing between scattering mechanisms. For a wind-roughened ocean surface, the scattering is dominated by a single dominant scattering mechanism, namely Bragg scattering ( $H \rightarrow 0$ ). In the presence of an oil slick, however, the entropy increases ( $H \rightarrow 1$ ) which is due to the number independent scattering mechanisms increasing due to damping of the small-scale Bragg waves. Comparison of entropy with the over flight observations indicated that the variability of the entropy was consistent with the variability of the oil properties suggesting that the entropy was providing a qualitative measure of the oil characteristics. Specifically, when there was open water and a thin sheen, the entropy was close to 0, but in the presence thicker oil due to the presence of, for example, an emulsion, the entropy had values that were close to 1.

**INTRODUCTION:**

Spaceborne radar has been used to monitor most of the major oil spills that have occurred using primarily single co-polarized data. False-positives notwithstanding, the radar data provides a good representation of the spatial extent of an oil spill, but there is usually limited information about inter-slick variability, i.e. sheen versus emulsion. The discrimination of sheen versus emulsion is important since in general sheen is non-recoverable, but emulsion can be recovered. Therefore, if sheen and emulsion can be discriminated, this information can be used to direct clean-up efforts in an efficient manner.

Single channel co-polarized radar imagery is acquired in horizontal (HH) or vertical (VV) polarization, where HH (VV) refers to the transmit and receive orientation of the radar wave. It is widely understood that the oil-water backscatter difference for VV polarization is slightly larger than for HH polarization, hence VV polarization is commonly used for oil slick detection. Work by MDA (2011) indicated that the Cloude-Pottier entropy parameter was sensitive to variations of surface-slick properties. Specifically the entropy was sensitive to variations in relative thickness, where relative thickness was due to the presence of sheen or emulsion on the ocean surface.

The entropy cannot be obtained from single co-polarized radar data, but requires quad-polarized data. Quad-polarized data means that the radar acquires two co-polarized channels (HH and VV) and two cross-polarized channels (HV and VH), but equally as important, quad-polarized data are phase-preserving meaning that the interchannel phase difference (e.g. phase difference between HH and VV) is available. The 2011 MDA study was based on a limited data set, so to further test the application of entropy for oil slick characterization, RADARSAT-2 quad-polarized imagery was acquired during the 2010 Macondo spill in the Gulf of Mexico. The RADARSAT-2 imagery was acquired over the spill site and the coastal areas (Figure 1). The objective of this study was to compare the variability of the entropy with aerial observations of the oil slick properties with the aim to assess the application of RADARSAT-2 quad-polarized data for oil slick characterization.

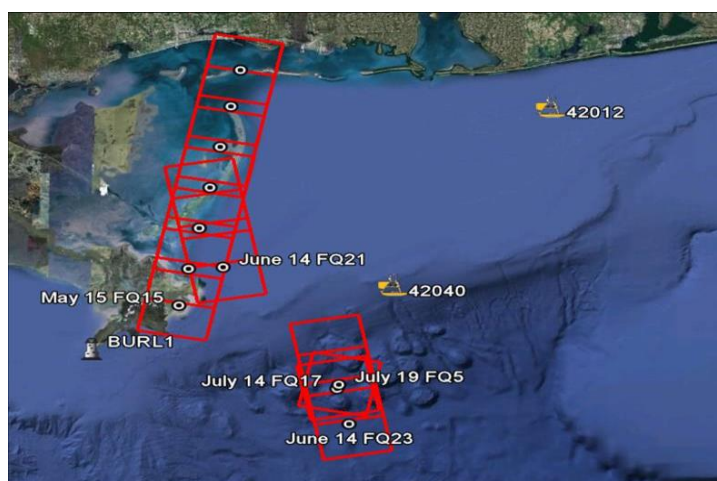


**Figure 1.** RADARSAT-2 quad-polarized acquisitions of the Macondo oil spill. 42040 and 42012 are the location of offshore buoys that provided wind speed.

The outline of this paper is as follows. Section 2 outlines the key radar parameters that influence oil slick detection in the ocean surface. Section 3 outlines the RADARSAT-2 data that was acquired and the use of the Oil Spill Situation Maps. Section 3 also provided an overview of the Cloude-Pottier entropy. Section 4 describes the results of the study and Section 5 provides a summary.

**OIL SLICK DETECTION:**

The detection of oil on the ocean surface requires discrimination between the ocean-surface backscatter and the backscatter from the oil. Scattering from the ocean-surface at incidence angles larger than about  $20^\circ$  is predominantly due to Bragg scattering from capillary waves and short gravity waves (Ulaby *et al.*, 1986). Oil spill detection using C-band radar has been demonstrated and validated using RADARSAT and ENVISAT (MDA, 2012, MDA, 2011; Solberg *et al.*, 2004; Indregard *et al.*, 2004; Brekke and Solberg, 2005, Solberg *et al.*, 1999; Staples and Hodgins, 1998). These studies suggest a range of incidence angles, wind speeds, and polarizations that are optimal for oil slick detection based on the presence of a slick.

Two of the three key-parameters that define ocean-surface backscatter are wind speed and SAR incidence angle: the backscatter increases with increasing wind speed, and decreases with increasing incidence angle. The detection of oil is enhanced at small incidence angles and for wind speeds roughly between 3 m/s and 12 m/s (Garcia-Pineda *et al.*, 2009; Brekke and Solberg, 2005; Ivanov *et al.* 2002; Staples and Hodgins, 1998). When wind speeds are low, the ocean-surface appears smooth relative to the SAR wavelength, and hence the backscatter is similar to the backscatter from the oil. When wind speeds are high, oil-induced attenuation is dominated by wind-induced surface roughness. Therefore, oil detection is optimal at moderate wind speeds, but can be problematic at low and high wind speeds.

A third parameter that dictates SAR oil detection is the polarization state of the radar. It is generally accepted that the co-polarization state, VV, provides stronger backscatter from the ocean surface than HH polarization. Cross-polarized radar returns (HV or VH) from the ocean surface are inherently low relative to returns from terrestrial targets or targets on the ocean surface such as ships and ice. At larger incidence angles and for low-wind conditions, ocean surface backscatter is close to the RADARSAT-2 noise floor. The noise floor does, however, vary for a given RADARSAT-2 beam modes (MDA, 2009), so the use of cross polarized modes depend on radar imaging parameters, beam mode, and environmental conditions.

**METHODOLOGY:****Data Acquisition**

RADARSAT-2 Fine Quad imagery was acquired over the Macondo oil spill between May 15, 2010 and July 19, 2010. In addition, wind speed was obtained from offshore buoys maintained by the National Data Buoy Centre (<http://ndbc.noaa.gov>). Of the five image acquisition dates, the July 14 image (Figure 2) was selected for analysis due to favorable wind conditions ( $\sim 4.5$  m/s) and time difference of less than six hours between aerial observations (see Section 3.2) and image acquisition.

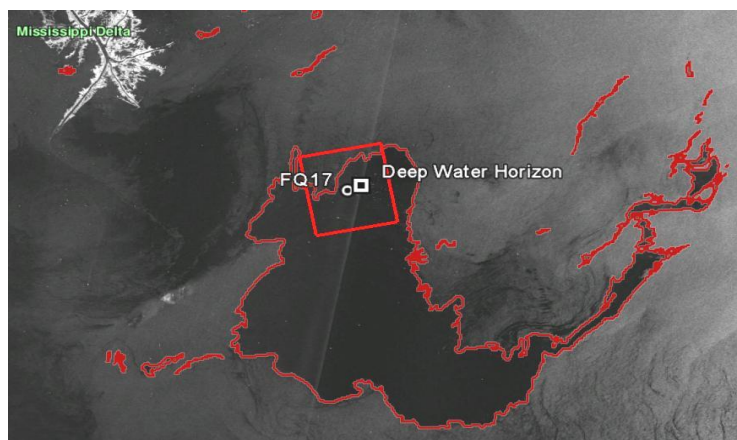


**Figure 2** The July 14, 2010 RADARSAT-2 acquisition (red coloured box) showing the spatial extent of the oil spill and the location of the Deep Water Horizon offshore platform. The oil spill extent was derived from ScanSAR imagery acquired a few hours before the Fine Quad acquisitions.

### Oil Spill Situation Maps

Oil spill situation maps were acquired to coincide with the RADARSAT coverage during the same period. These maps were based on observations from aircraft and other *in situ* data. An example of an oil spill situation map for July 14 is shown in Figure 3. The location of the Deep Water Horizon platform and the approximate scene-centre of the RADARSAT-2 image is indicated. The situation maps provide the spatial extent of the oil spill based on previous-day data and an estimate of the projected oil-spill extent based on numerical models. In addition, the situation maps provide information on the state of the oil (e.g. sheen versus brown oil) and observations on the presence of algae (see Overflight Observations in Figure 3).

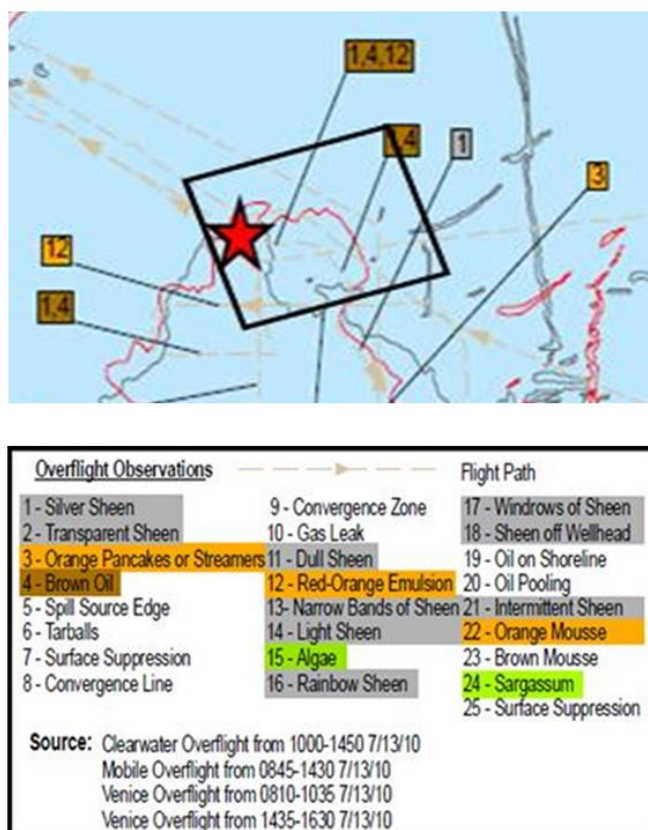


**Figure 3 Oil Spill Situation map issued on July 14 derived from airborne observations from July 13. The spill source is indicated by the red-coloured star. The spatial extent of the RADARSAT-2 acquisition is indicated by the black-coloured box. Adapted from <http://gomex.erma.noaa.gov>**

### Cloude-Pottier Decomposition

The Cloude-Pottier decomposition algorithm is based on an eigen decomposition of the coherency matrix, which decomposes the coherency matrix into three orthogonal scattering mechanisms, namely the entropy, anisotropy, and the alpha-angle (Cloude and Pottier, 1996). One of the Cloude-Pottier decomposition parameters, the entropy ( $0 \leq H \leq 1$ ), provides a measure of the amount of mixing between scattering mechanisms. A value of zero indicates a single dominant scattering mechanism (single non-zero eigenvalue) and a value of one indicates an equal mixture of three scattering mechanisms (equal eigenvalues).

For a wind-roughened ocean surface, the scattering is dominated by a single dominant scattering mechanisms, namely Bragg scattering ( $H \rightarrow 0$ ). In the presence of an oil slick, however, the entropy increases ( $H \rightarrow 1$ ) which is due to the number independent scattering mechanisms increasing due to damping of the small-scale Bragg waves. At small incidence angles ( $< \sim 30^\circ$ ), the entropy for the ocean and the oil are similar. As the incidence angle increases, however, the oil entropy increases with incidence angle, but the ocean entropy remains relatively constant (MDA, 2011; Migliaccio *et al.* 2007; Shuler and Lee, 2004).

In the region between imaging slick-free water and an oil slick, the entropy is expected to vary as a function of the properties of the oil. While there are many oil properties, the variability of these properties must, at some level, change the ocean surface roughness in such a manner that there is a measurable change in the radar backscatter

## RESULTS:

Observation of oil types were derived from the Oil Spill Situation Maps based on aerial overflights and overlaid on the July 14 entropy image (Figure 4), with the oil types listed in Table 1. Given the time difference between the quad-polarized data acquisition and the overflight observations, the exact location of the observation was difficult to know. Further, there were inherent errors in the locations from the overflight observer. With these errors in mind, it was the general properties of the entropy versus the actual entropy value at a given location that was assessed.

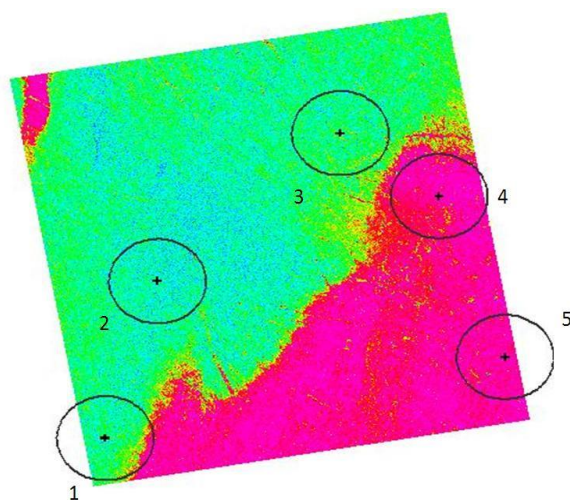


**Figure 4** Entropy from the July 14 image. Low entropy is blue and high entropy is magenta. The five areas are overflight observations of oil type. The circles are a buffer zone with a 3 km radius.

**Table 1** Oil type observations that coincide with the July 14 quad-polarized image. The oil types were obtained from the Oil Spill Situation Maps.

Location	Oil Type Observed
1 and 2	Silver Sheen
3	Silver Sheen, Red-Orange Emulsion
4 and 5	Silver Sheen, Brown Oil, Red-Orange Emulsion

The oil types for locations 1 – 5 are shown in Figure 5. The entropy varies from about 0.2 (blue-coloured region) to about 0.9 (magenta-coloured region). Low entropy has been associated with relatively oil-free water and high entropy occurs in the presence of oil: the variation of the July 14 entropy appears consistent with this observation. Locations 1 and 2 had silver sheen (thin oil), so the presence of the sheen should cause an increase in the entropy. Location 3 had silver sheen and red-orange emulsion. In general the emulsion is thicker than the silver sheen (Gillot *et al.*, 1988), so the increased thickness should increase ocean-surface damping and hence increase the entropy. Locations 4 and 5 had the same oil types as location 3 plus the addition of brown oil.

Locations 4 and 5 were in the main part of the oil slick, so an entropy increase was expected. However, the variation of the observed oil type for each location suggests that the variability of the entropy was in response to the variability of the oil type. For example, location 1 was not in the main part of the slick, so there is a combination of clear water and some oil. In contrast, location 4 was in the main part of the slick, so the entropy increased, but within the main oil slick, there was variability of the entropy once again suggesting the entropy is providing a measure of the variability of the oil.



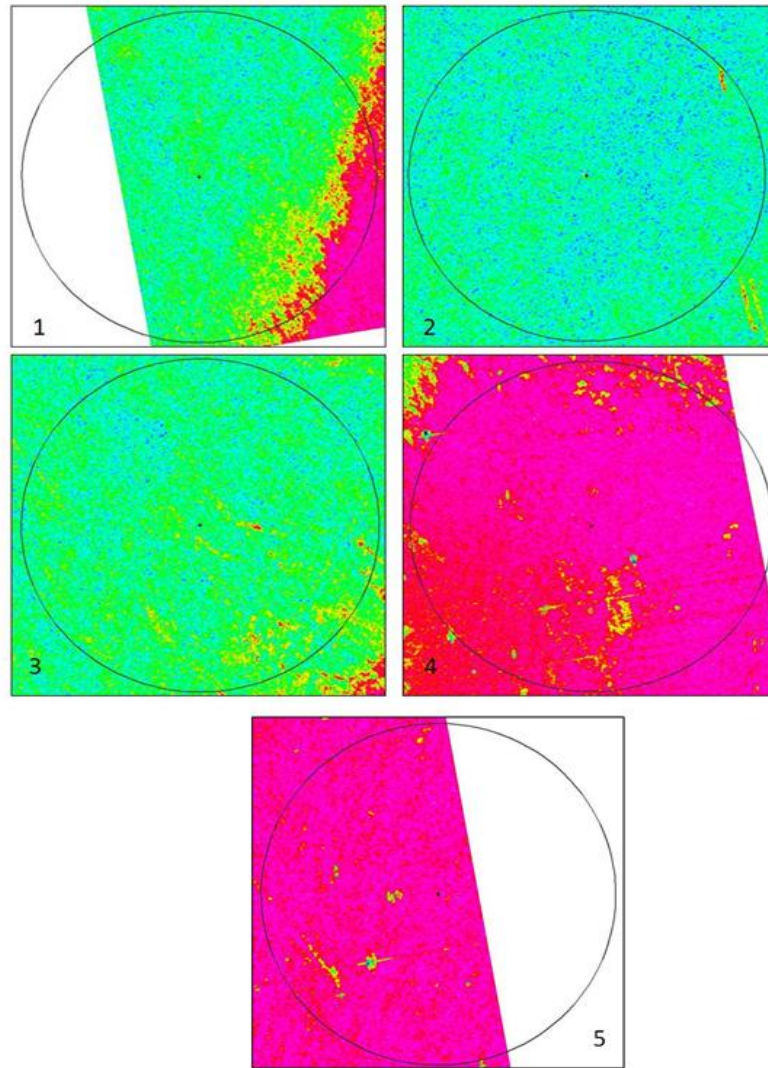


Figure 5. Entropy for the locations 1-5. The entropy values from about 0.2 (blue) to 0.9 (magenta).

### SUMMARY:

The Cloude-Pottier entropy, derived from RADARSAT-2 quad-polarized imagery, was used to assess the slick characteristics from the Macondo oil spill. The entropy provides a measure of the amount of mixing between scattering mechanisms. For a wind-roughened ocean surface, the scattering is dominated by a single dominant scattering mechanisms, namely Bragg scattering ( $H \rightarrow 0$ ). In the presence of an oil slick, however, the entropy increases ( $H \rightarrow 1$ ) which is due to the number independent scattering mechanisms increasing due to damping of the small-scale Bragg waves. The variability of the entropy was due to differential damping based on the different oil characteristics.



## 2014 INTERNATIONAL OIL SPILL CONFERENCE

During the Macondo oil spill, Oil Spill Situation Maps were produced on a daily basis. These Maps provided information on the spatial extent of the oil spill and location-specific observations of the oil properties (e.g. presence of sheen, emulsion) based on airborne overflights. Wind speed and direction were obtained by offshore buoys in vicinity of the spill. The location-specific overflight observations were compared to the results from the polarimetric analysis.

Comparison of entropy derived from the July 14 image with the overflight observations indicated that the variability of the entropy was consistent with the variability of the oil properties suggesting that the entropy was providing a qualitative measure of the oil characteristics. Specifically, when there was open water and a thin sheen, the entropy was close to 0, but in the presence of thicker oil due to the presence of, for example, an emulsion, the entropy had values that were close to 1.

---

Figure-1, 2, 4 and 5 Image copyright: RADARSAT-2 Data and Products © MacDonald, Dettwiler and

Associates Ltd (2010). All Rights Reserved. RADARSAT is an official mark of the Canadian Space Agency.

## REFERENCES:

- Brekke, C. and Solberg, A.H.S., 2005. Oil spill detection by satellite remote sensing, *Remote Sensing of Environment*, Vol. 95, No. 1, pp 1-13.
- Cloude, S.R. and Pottier, E., 1996. A Review of Target Decomposition Theorems in Radar Polarimetry, *IEEE Transactions on Geoscience and Remote Sensing*, Vol. 34, No. 2, pp 498-518.
- Garcia-Pineda, O., Zimmer, B., Howard, M., Pichel, W., Xiaofeng, L., and I. MacDonald, Using SAR Images to Delineate Ocean Oil Slicks with a Texture-Classifying Neural Network Algorithm (TCNNA), *Can. J. of Rem. Sens*, 35(5), 2009.
- Gillot, A., G.H.R. Aston, P. Bonanzinga, Y. le Gal la Salle, M.J. Mason, M.J. O'Neill, J.K. Rudd and D.I. Stonor., 1988, Field guide to application of dispersants to oil spills. Rept No.2/88. The Hague, Netherlands, 64 pp..
- Indregard, M., Solberg, A., Clayton, P., 2004. D2-report on benchmarking oil spill recognition approaches and best practice. Tech. rep., Oceanides project, European Commission, Archive No. 04-10225-A-Doc, Contract No: EVK2-CT-2003-00177.
- Ivanov, A. He, M.-X. and Fang, M.-Q. (2002). Oil Spill Detection with the RADARSAT SAR in the Waters of the Yellow and East China Sea: A Case Study. 23<sup>rd</sup> Asian Conference on Remote Sensing. Kathmandu, Nepal. 25-29 November.
- MDA, Offshore Angola Oil Seep Analysis, RV-01-5283, October 2012.
- MDA, Marine Environmental Surveillance Improvements with RADARSAT-2, Final report, P-191, March 2011
- MDA, RADARSAT-2 SAR Calibration and Characterization Report, **RN-RP-52-6759**, March 2009.
- Migliaccio, M., Gambardella, A., and Tranfaglia, M., 2007. SAR polarimetry to observer oil spills. *IEEE Trans. Geoscience and Remote Sensing* vol. 45, no. 2, pp. 506-511.
- Shuler, D. and J. Lee, Polarimetric SAR Studies of Ocean Surface Features using Orientation Angles and Parameters of the H/A/ $\alpha$  Decomposition, May 2004, *Proceedings EUSAR*, Elm, Germany.
- Solberg, A.H.S., Brekke, C., Solberg, R., Husøy, P.O., 2004. Algorithms for oil spill detection in RADARSAT and ENVISAT SAR images. *Proc. IGARSS'04*, pp 4909–4912
- Solberg, A.H.S., Storvik, G., Solberg, R. and Volden, E., 1999. Automatic Detection of Oil Spills in ERS SAR Images, *IEEE Transactions on Geoscience and Remote Sensing*, Vol. 37, No. 4, pp 1916-1924.

300300

2014 INTERNATIONAL OIL SPILL CONFERENCE

Staples, G.C., and D.O. Hodgins, RADARSAT-1 Emergency Response for Oil Spill Monitoring, *Proceedings Fifth Int'l. Conf. on Rem. Sens. for Marine and Coastal Environments*, October, 1998.

Ulaby F., Moore, R. and A. Fung, Microwave Remote Sensing, Vol. 3, 1986, Artec House, Norwood, MA.